Supplemental Information

Three-dimensional microporous and mesoporous covalent organic frameworks based on cubic building units

Li Liao, Xinyu Guan, Haorui Zheng, Zerong Zhang, Yaozu Liu, Hui Li, Liangkui Zhu, Shilun Qiu, Xiangdong Yao,* and Qianrong Fang**

Table of contents

Section S1. Materials and characterization

S1.1 Materials

All starting materials and solvents, unless otherwise noted, were obtained from J&K scientific LTD and used without further purification. All products were isolated and handled under nitrogen using either glovebox or Schlenk line techniques.

S1.2 Instruments

A Bruker AV-400 NMR spectrometer was applied to record the liquid ^{1}H NMR spectra. Solid-state ^{13}C NMR spectra were recorded on an AVIII 500 MHz solid-state NMR spectrometer. The FTIR spectra (KBr) were obtained using a SHIMADZU IRAffinity-1 Fourier transform infrared spectrophotometer. A SHIMADZU UV-2450 spectrophotometer was used for all absorbance measurements. Thermogravimetric analysis (TGA) was recorded on a SHIMADZU DTG-60 thermal analyzer under N_2. The operational range of the instrument was from 30 °C to 800 °C at a heating rate of 10 °C min^{-1} with N_2 flow rate of 30 mL min^{-1}. PXRD data were collected on a PANalytical B.V. Empyrean powder diffractometer using a Cu Kα source (λ = 1.5418 Å) over the range of 2θ = 2.0−40.0° with a step size of 0.02° and 2 s per step. The sorption isotherm for N_2 was measured by using a Quantachrome Autosorb-IQ analyzer with ultra-high-purity gas (99.999% purity). To estimate pore size distributions for JUC-588 and JUC-589, nonlocal density functional theory (NLDFT) was applied to analyze the N_2 isotherm on the basis of the model of N_2@77K on carbon with slit pores and the method of non-negative regularization. For scanning electron microscopy (SEM) image, JEOL JSM-6700 scanning electron microscope was applied. Transmission electron microscopy (TEM) image was obtained on JEM-2100 transmission electron microscopy.

S1.3 Synthesis of 5-(4,4,5,5-tetramethyl-1,3,2-dioxaborolan-2-yl)isophthalaldehyde[1]

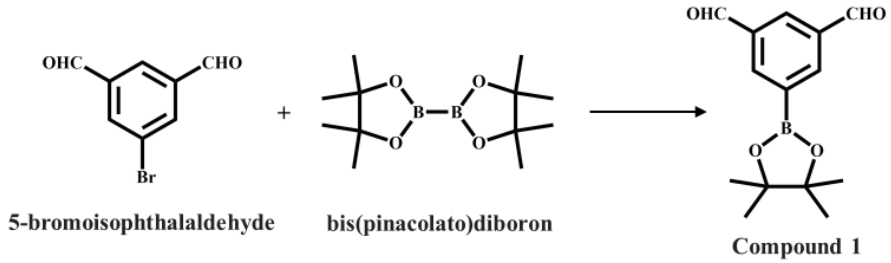

5-bromoisophthalaldehyde bis(pinacolato)diboron Compound 1

To a solution of 5-bromoisophthalaldehyde (15.0 g, 70.4 mmol, 1.0 eq.), bis(pinacolato)diboron (19.7g, 77.4 mmol, 1.1 eq.) and KOAc (20.7 g, 211.2 mmol, 3.0 eq.) in anhydrous 1,4-dioxane (100 mL), $Pd(dppf)Cl_2$ (1.54 g, 2.11 mmol, 0.03 eq.) was added. The reaction was heated to 90 °C and stirred for 16 h. The solid precipitate was filtered off and washed with Et_2O. The filtrate was washed with water (100 mL) and brine (100 mL), dried over $MgSO_4$ and evaporated to dryness. The residue was dissolved in DCM and purified by flash chromatography on silica gel, eluting with a 0 to 50% EtOAc in DCM gradient. Likely fractions were evaporated in vacuo, affording the 5-(4,4,5,5-tetramethyl-1,3,2-dioxaborolan-2-yl)isophthalaldehyde (Compound 1) as an oil that solidifies on standing (15.9 g, 61.2 mmol, 87%). ^{1}H NMR (500 MHZ, $CDCl_3$): δ = 10.11 (s, 2 H), 8.54 (d, 2 H, J = 1.7 Hz), 8.44 (t, 1 H, J = 1.7 Hz), 1.36 (s, 12 H). HRMS-Cl: calcd. for $C_{14}H_{18}BO_4$ $[M+1]^+$ 260.1329, found 260.1319.

S1.4 Synthesis of 3,3′,5,5′-Tetraethynyl-2,2′,6,6′-tetramethoxy-4,4′-dimethylbiphenyl[2,3]

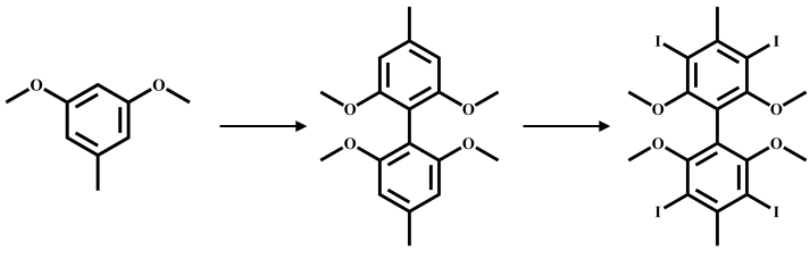

3,5-dimethoxytoluene Compound 2 Compound 3

Synthesis of Compound 2: nBuLi (20 mL, 22 mmol, 2.2 M in hexane) was added to a mixture of 3,5-dimethoxytoluene (3.04 g, 20 mmol) and tetramethylethylenediamine (2.78 g, 24 mmol) in dry THF (50 mL) at –78 °C. After stirring for 5 min at –78 °C, the temperature was raised to 0 °C. 2.5 h later, $FeCl_3$ (3.88 g, 24 mmol) was added in portions and then the reaction mixture was warmed to room temperature. After stirring for 8 h at room temperature, HCl (ca. 50 mL,

1 M) was added and the mixture was extracted with ethyl acetate (50 mL × 3). The organic layers were dried with anhydrous Na_2SO_4. After evaporation under reduced pressure, the residue was washed with hexane to give the Compound 2 (1.9 g, 65 % yield). ^{1}H NMR ($CDCl_3$): δ = 6.47 (s, 4 H); 3.70 (s, 12 H); 2.38 (s, 6 H) ppm. ^{13}C NMR ($CDCl_3$): δ = 158.23,138.65, 109.57, 105.58, 56.12, 22.33 ppm.

Synthesis of Compound 3: To a mixture of Compound 2 (2.0 g, 6.6 mmol), solid iodine (3.5 g, 13.5 mmol), and $HIO_4{\cdot}_2H_2O$ (1.55 g, 6.7 mmol) in a 250 mL flask, $CH_3COOH/H_2O/H_2SO_4$ (120/24/3.6 mL) was added. The resulting mixture was stirred at 120 °C for 3 days. After it was cooled down to room temperature, the reaction mixture was diluted with 250 mL of water. The precipitate was filtered and washed with water. The pink solid was dissolved in 100 mL of $CHCl_3$ and washed with saturated $Na_2S_2O_3$ solution to remove iodine residue. The $CHCl_3$ phase was evaporated to ca. 20 mL under reduced pressure, and then, 100 mL of methanol was added. 3,3′,5,5′-Tetraethynyl-2,2′,6,6′-tetramethoxy-4,4′-dimethylbiphenyl (Compound 3) was collected as a white solid (4.8 g, 90% yield). ^{1}H NMR (300 MHz, $CDCl_3$) δ = 3.58 (s, 12 H), 2.96 (s, 6 H). ^{13}C NMR (75 MHz, $CDCl_3$) δ = 158.5, 145.6, 121.0, 93.1, 60.8, 36.4 ppm.

S1.5 Synthesis of BDFTM

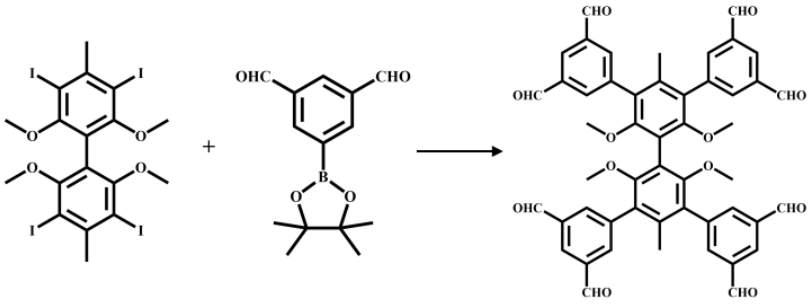

Compound 3 Compound 1 BDFTM

To a flask containing 1,4-Dioxane/H_2O (80 mL/8 mL), Compound 3 (1.52 g, 1.9 mmol), Compound 1 (3.5 g, 15.1 mmol), palladium tetrakis(triphenylphosphine) (0.2 g, 0.2 mmol), and cesium carbonate (4.9 g, 15.0 mmol) were added. The mixture was heated under nitrogen at 90 ℃ for 3 days. After cooling to room temperature, the solvent was removed under reduced pressure. Then the residues were dissolved in ethylacetate, washed with water and brine, and dried over anhydrous Na_2SO_4. After that, the solvent was evaporated under reduced pressure and the crude product was purified by column chromatography to yield BDFTM as a

white solid (75% yield). ^{1}H NMR (400 MHz, $CDCl_3$, ppm): δ = 10.17. (s, 8 H), 8.41 (t, J = 1.6 Hz, 4 H), 8.14 (d, J = 1.6 Hz, 8 H), 3.3 (s, 12 H), 1.88 (s, 6 H). ^{13}C NMR (100 MHz, $CDCl_3$) δ = 190.20, 156.03, 139.19, 136.54, 136.50, 135.5, 129.65, 129.12, 120.20, 60.71, 18.96 ppm.

S1.6 Synthesis of 4,4'-(9H-carbazole-3,6-diyl)dibenzaldehyde

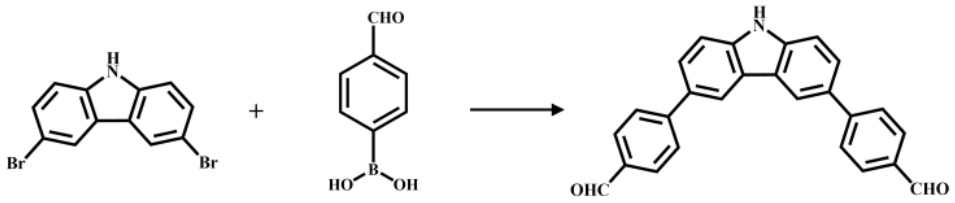

3,6-Dibromocarbazole 4-formylphenylboronic acid Compound 4

A mixture of 3,6-dibromocarbazole (975.0 mg, 3.0 mmol), (4-formylphenyl)boronic acid (1.13 g, 7.5 mmol), $Pd(PPh_3)_4$ (20 mg), 1,4-Dioxane (20 mL) and aqueous solution of K_2CO_3 (1 M, 20 mL) was refluxed at 90 °C overnight under N_2 atmosphere. Then the mixture was cooled down to room temperature. The solid was isolated by filtration, washed three times with ethyl acetate and then washed another three times with water. The residue was dissolved in DCM and purified by column chromatography to yield compound 4 as a yellow solid (73% yield). ^{1}H NMR (400 MHz, DMSO-*d*6): δ =11.60 (s, 1 H), 10.05 (s, 2 H), 8.784 (d, 2 H, J = 1.6 Hz), 8.036 (dd, 8 H, J_1 = 8 Hz, J_2 = 8 Hz), 7.87 (dd, 2 H, J_1 = 1.6 Hz, J_2 = 1.6 Hz), 7.63 (d, 2 H, J = 16 Hz). ^{13}C NMR (100 MHz, $CDCl_3$) δ = 192.30, 146.74, 140.35, 134.06, 129.38, 126.94, 126.52, 123.25, 118.52, 111.56 ppm.

S1.7 Synthesis of TBFPC

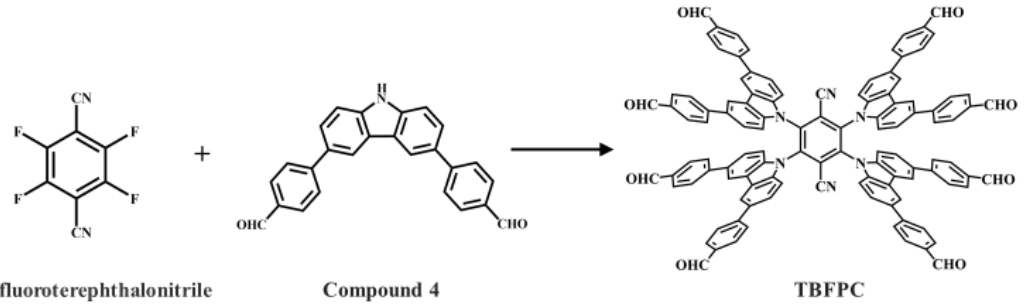

tetrafluoroterephthalonitrile Compound 4 TBFPC

Under a nitrogen atmosphere, Compound 4 (3.77 g, 10.5 mmol) was dissolved in dry THF (120mL). Upon sodium hydride (60% dispersion, 0.8 g, 20.0 mmol) being added, the color of the mixture turned yellow along with the production of a lot of gas. The suspension was stirred at room temperature for 30 min. After the subsequent addition of 2,3,5,6-

tetrafluoroterephthalonitrile (0.5 g, 2.5 mmol), the reaction mixture was stirred for 24h. Eventually, the color of the suspension converted from yellow to red. The suspension was separated through the suction filter to afford a red solid. The solid was then washed with water (100 mL × 3), THF (100 mL × 3) and dried in air to give the TBFPC (70% yield). ^{1}H NMR (400 MHz, DMSO-*d*6): δ = 10.064 (s, 1 H), 8.60 (s, 1 H), 8.115 (d, 1 H, J = 8 Hz), 7.972 (dd, 4 H, J_1 = 8 Hz, J_2 = 8 Hz), 7.80 (d, 1 H, J = 8 Hz). ^{13}C NMR (100 MHz, DMSO-*d*6) δ = 193.14, 146.41, 141.47, 140.42, 135.20, 133.09, 130.59, 127.77, 125.70, 124.88, 123.11, 120.23, 112.48 ppm.

S1.8 Synthesis of JUC-588

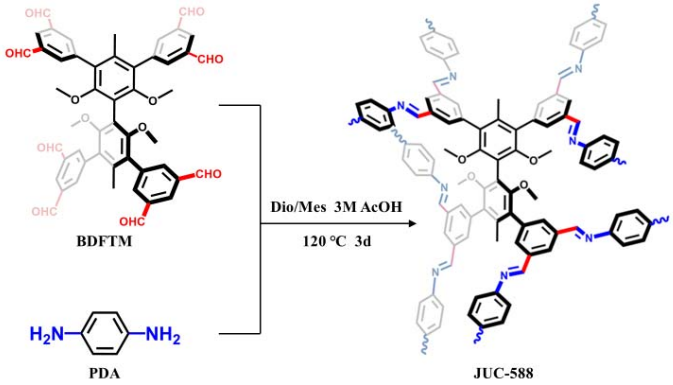

BDFTM (0.03 mmol, 24.9 mg) and PDA (0.12 mmol, 13.0 mg) were weighted into a Pyrex tube (volume: ca. 20.0 mL with a body length of 18.0 cm and neck length of 9.0 cm), and the mixture was added into 0.8 mL of dioxane, 0.2 mL of mesitylene and 0.1 mL of acetic acid (3 M). The Pyrex tube was flash frozen in a liquid nitrogen bath, evacuated to an internal pressure of ca. 19.0 mbar and flame-sealed, reducing the total length by ca. 10.0 cm. Upon warming to room temperature, the tube was placed in an oven at 120 °C for 3 d. The resulting precipitate was filtered, exhaustively washed by Soxhlet extractions with dioxane for 48 h. The obtained powder was immersed in anhydrous acetone, and the solvent was exchanged with fresh acetone for several times. The wet sample was then transfer to a super critical drier (Samdri-PTV-3D), in which the sample was washed with six times of liquid CO_2, and exchanged with fresh CO_2 for six times with the interval of half hour. The system was heat up to 45 ºC to bring about the supercritical state of the CO_2, which was bleed after half hour in very slow flow rate to ambient pressure. The sample was then transferred to vacuum chamber and evacuated to

20 mTorr under room temperature, yielding yellow powder for N_2 adsorption measurements. Anal. Cald: C: 81.02; H: 2.92; N: 10.22. Found: C: 81.10; H: 2.89; N: 10.30.

S1.9 Synthesis of JUC-589

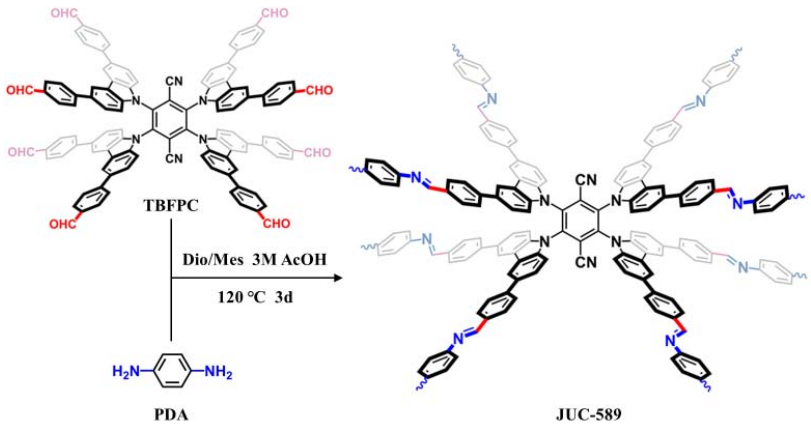

TBFPC (0.02 mmol, 32.4 mg) and PDA (0.08 mmol, 8.65 mg) were weighted into a Pyrex tube (volume: ca. 20.0 mL with a body length of 18.0 cm and neck length of 9.0 cm), and the mixture was added into 0.5 mL of dioxane, 0.5 mL of mesitylene and 0.1 mL of acetic acid (3 M). The Pyrex tube was flash frozen in a liquid nitrogen bath, evacuated to an internal pressure of ca. 19.0 mbar and flame-sealed, reducing the total length by ca. 10.0 cm. Upon warming to room temperature, the tube was placed in an oven at 120 °C for 3 d. The resulting precipitate was filtered, exhaustively washed by Soxhlet extractions with dioxane for 48 h. The obtained powder was immersed in anhydrous acetone, and the solvent was exchanged with fresh acetone for several times. The wet sample was then transfer to a super critical drier (Samdri-PTV-3D), in which the sample was washed with six times of liquid CO_2, and exchanged with fresh CO_2 for six times with the interval of half hour. The system was heat up to 45 ºC to bring about the supercritical state of the CO_2, which was bleed after half hour in very slow flow rate to ambient pressure. The sample was then transferred to vacuum chamber and evacuated to 20 mTorr under room temperature, yielding red powder for N_2 adsorption measurements. Anal. Cald: C: 85.55; H: 4.19; N: 10.26. Found: C: 85.49; H: 4.23; N: 10.28.

Section S2. SEM images

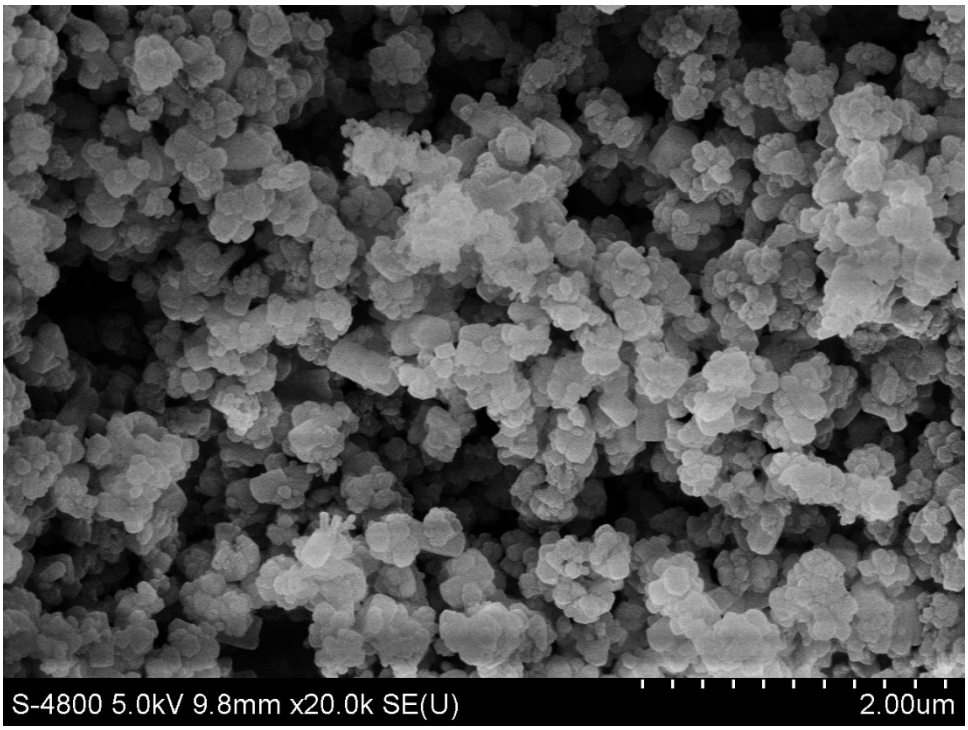

Figure S1. SEM image of JUC-588.

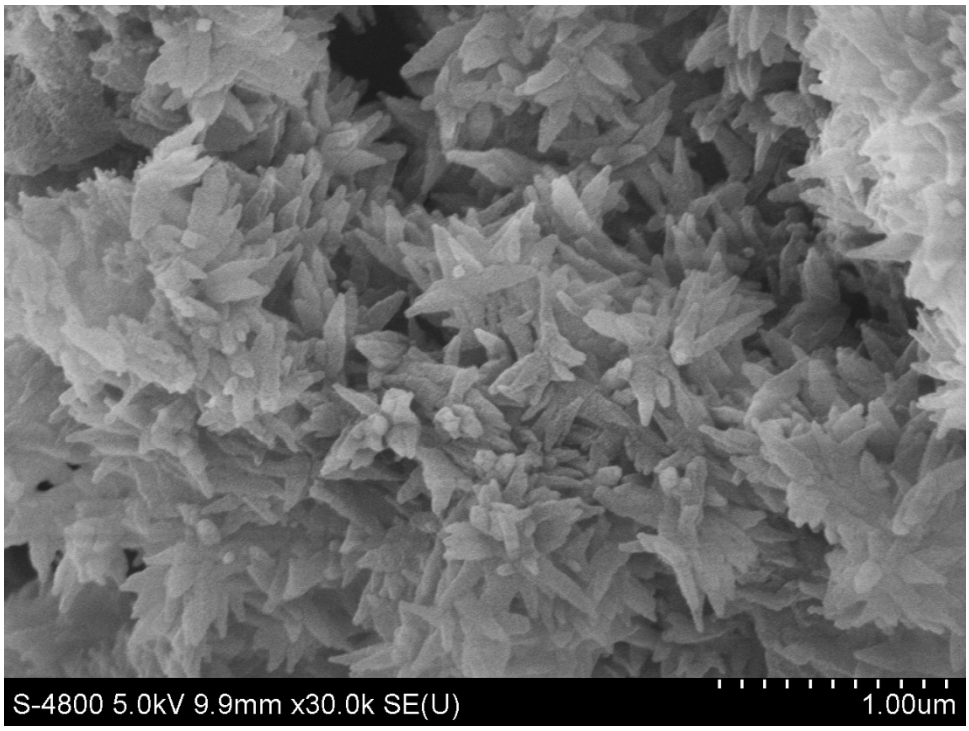

Figure S2. SEM image of JUC-589.

Section S3. TEM images

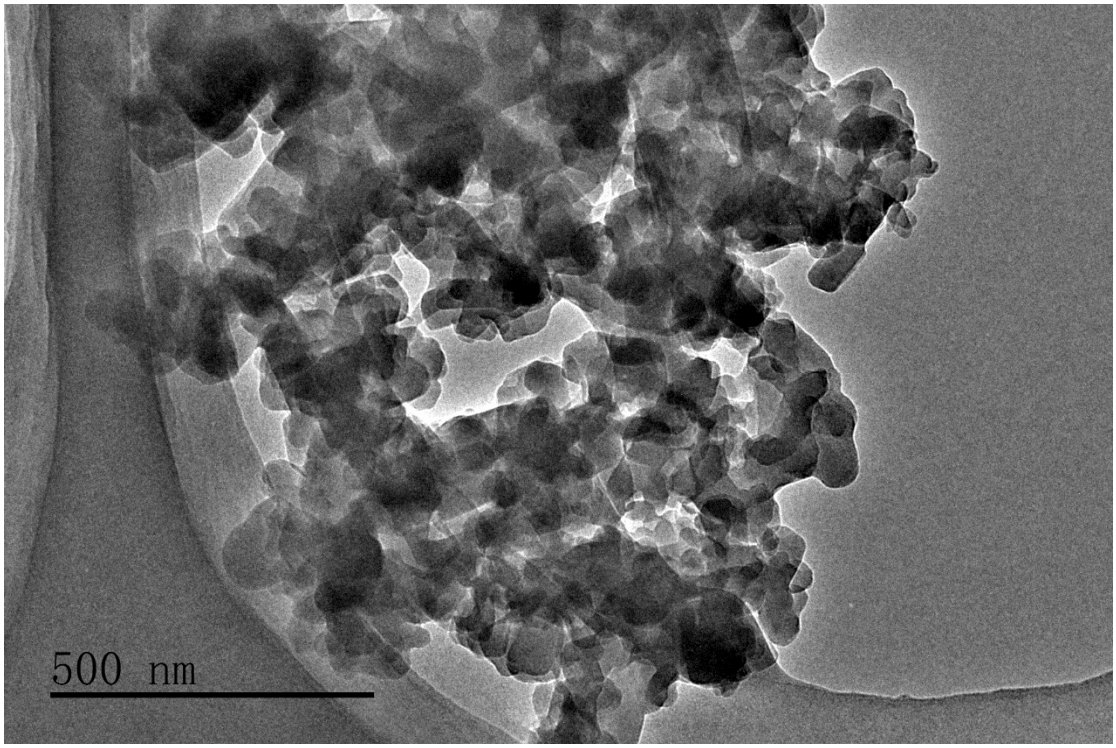

Figure S3. TEM image of JUC-588.

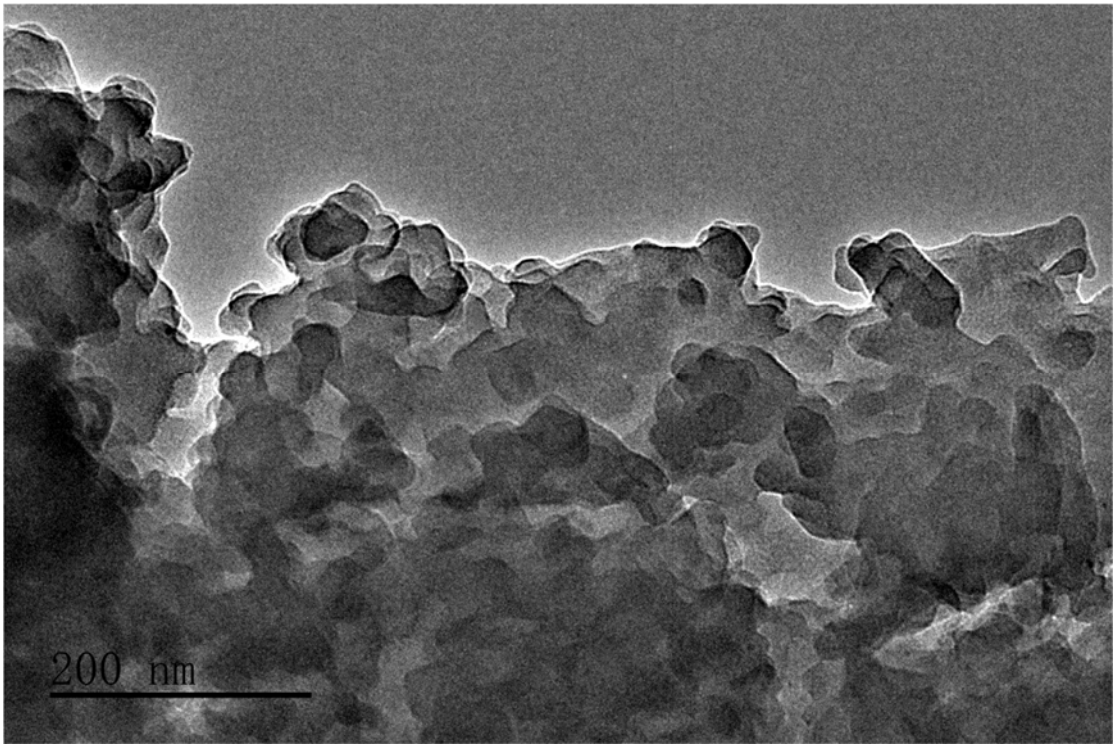

Figure S4. TEM image of JUC-589.

Section S4. FT-IR spectra

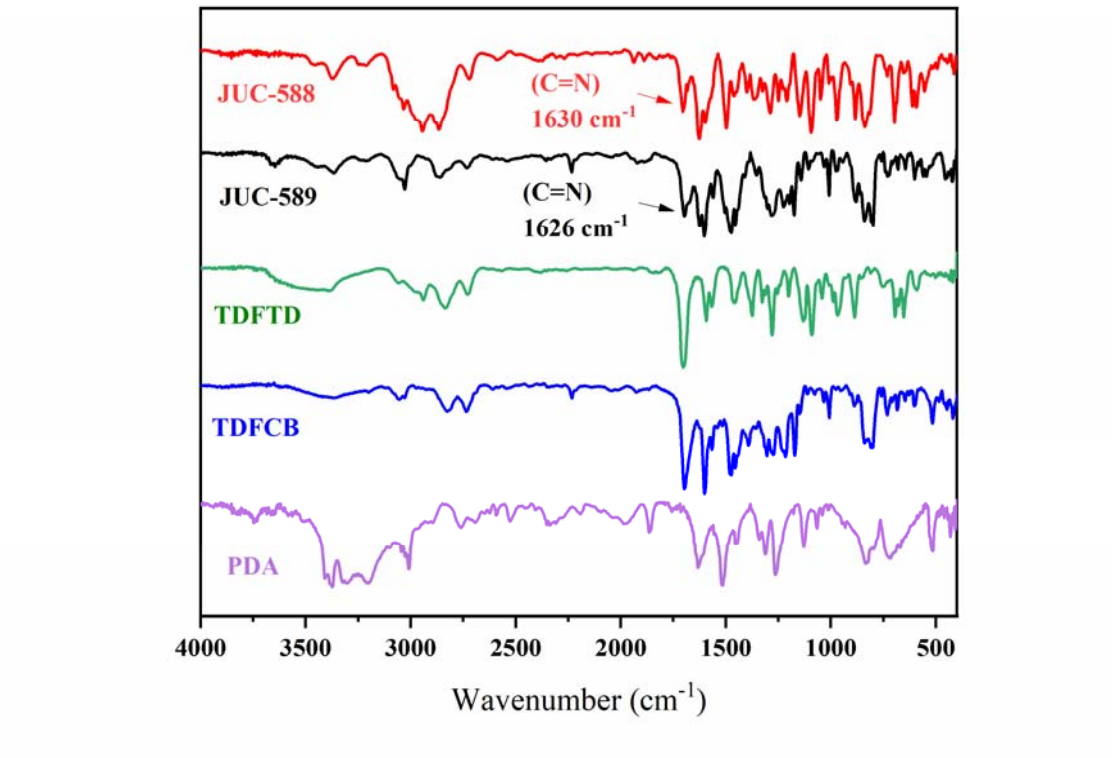

Figure S5. FT-IR spectra of JUC-588 (red) and JUC-589 (black), TDFTD (green), TDFCB (blue), PDA (purple).

Section S5. NMR spectra

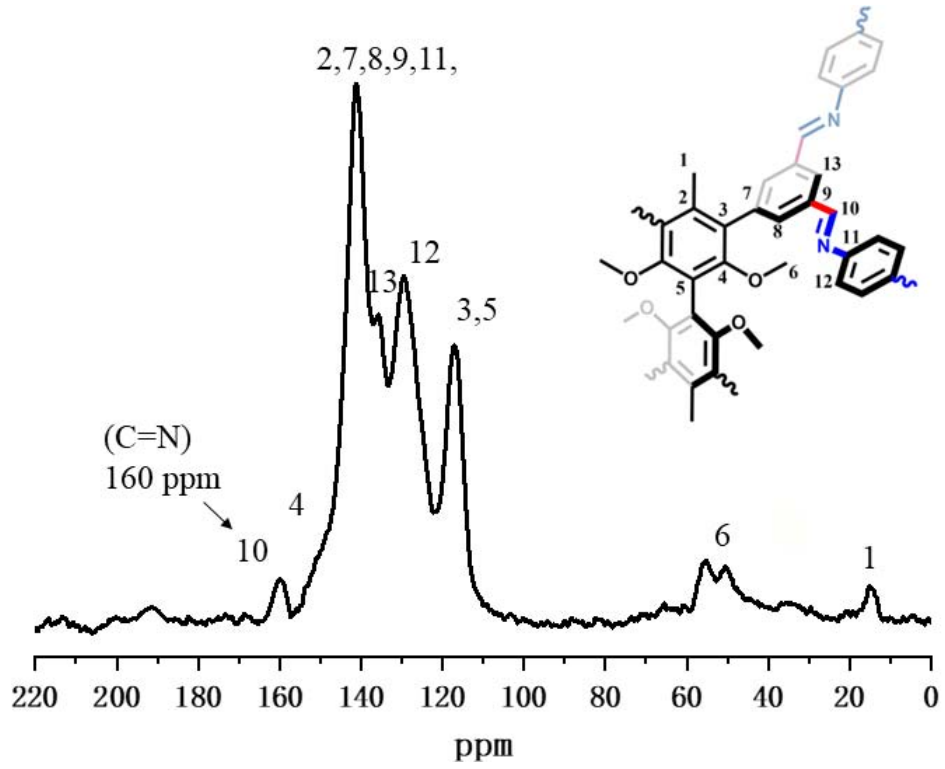

Figure S6. Solid state ^{13}C NMR of JUC-588.

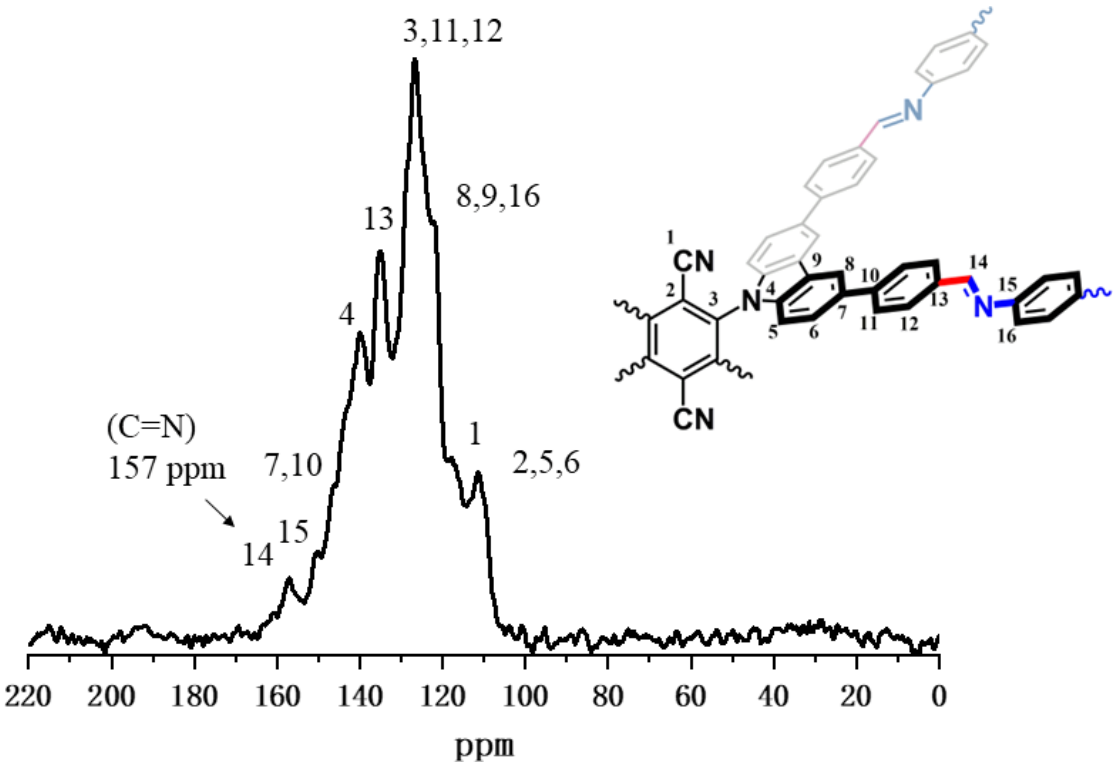

Figure S7. Solid state ^{13}C NMR of JUC-589.

Section S6. TGA curves

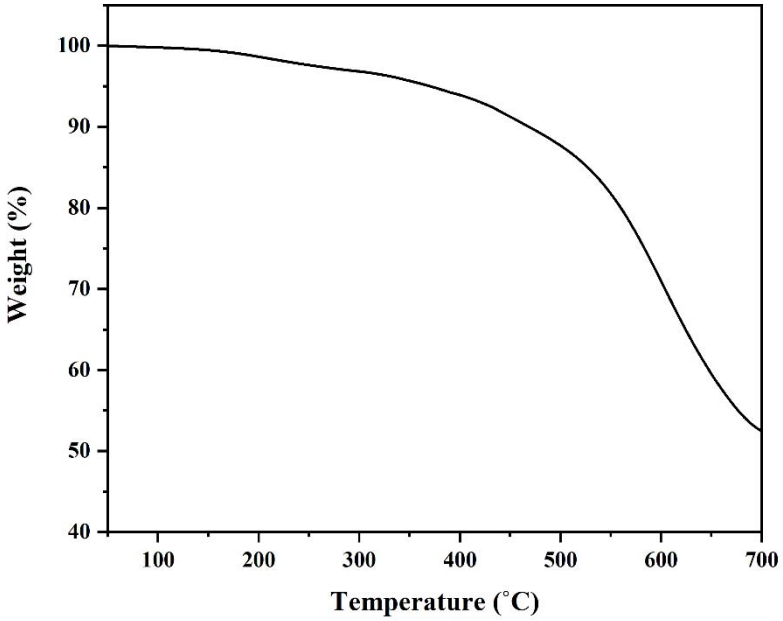

Figure S8. TGA curve of JUC-588.

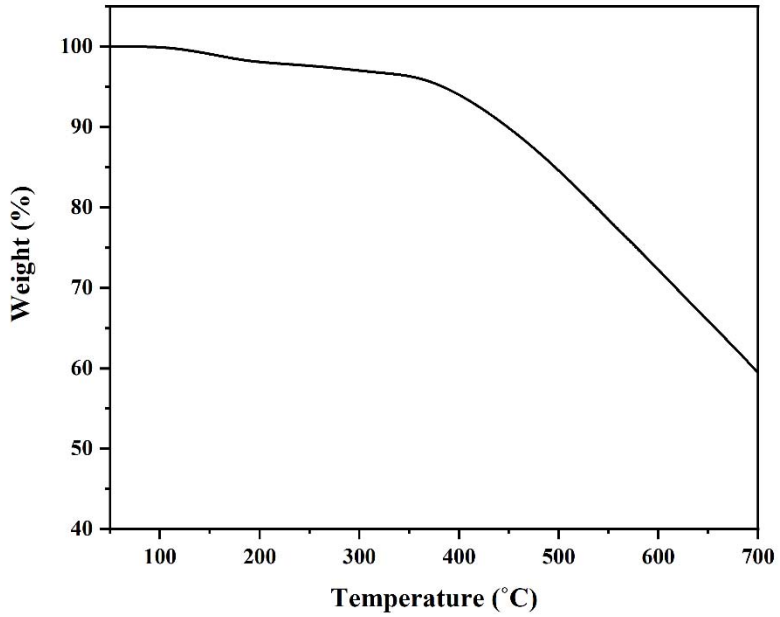

Figure S9. TGA curve of JUC-589.

Section S7. Chemical stability

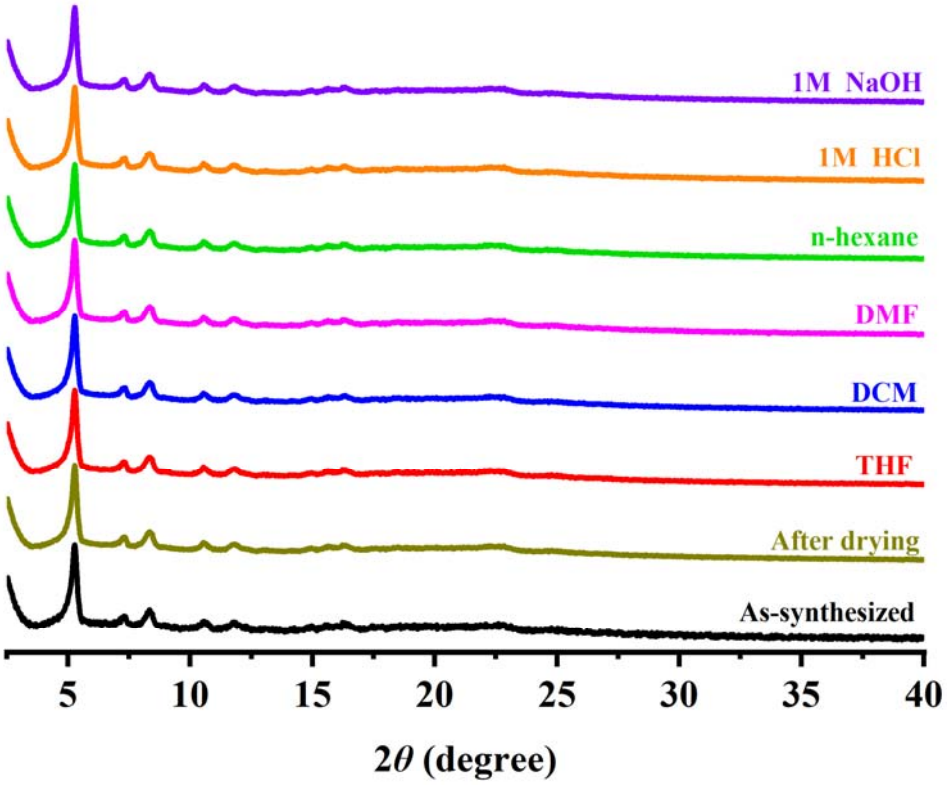

Figure S10. PXRD patterns of JUC-588 after 72 h treatment in different solvents and drying.

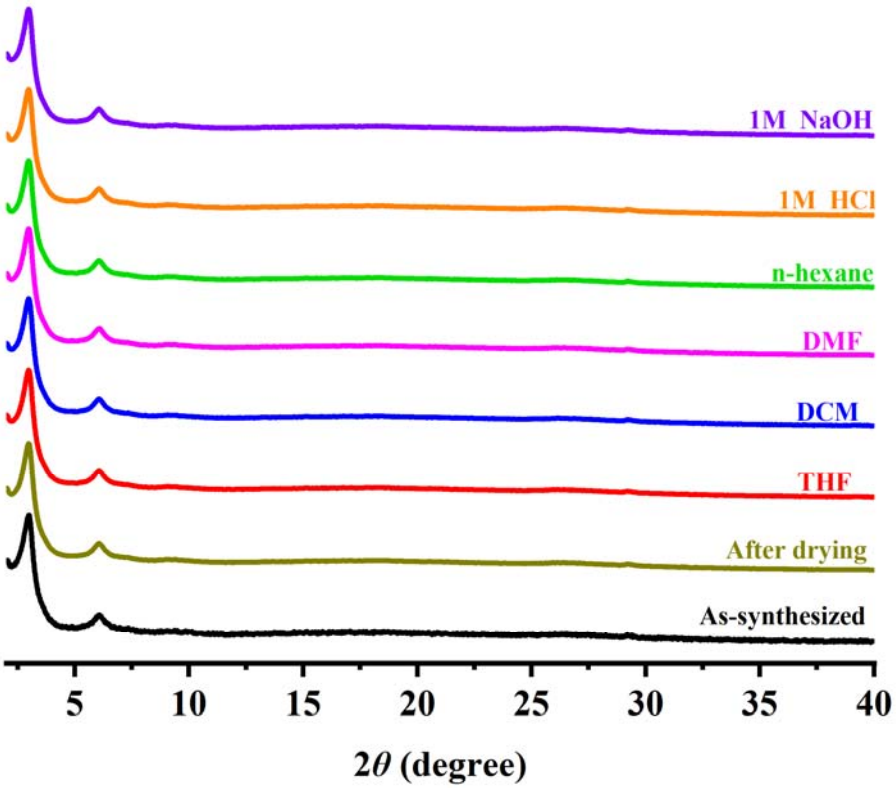

Figure S11. PXRD patterns of JUC-589 after 72 h treatment in different solvents and drying.

Section S8. PXRD patterns

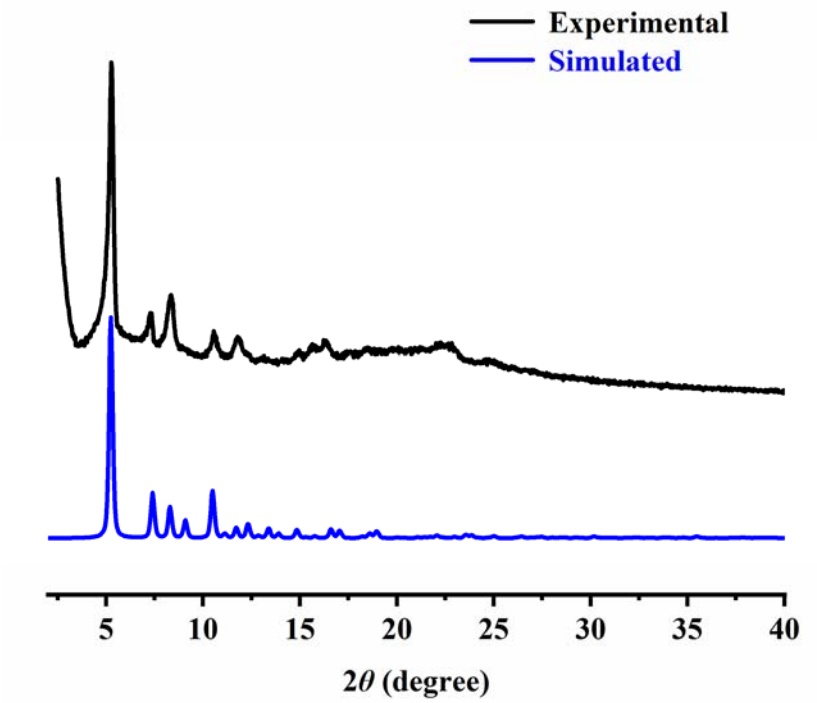

Figure S12. A comparison of experimental and simulated PXRD patterns of JUC-588 based on the **bcu** net.

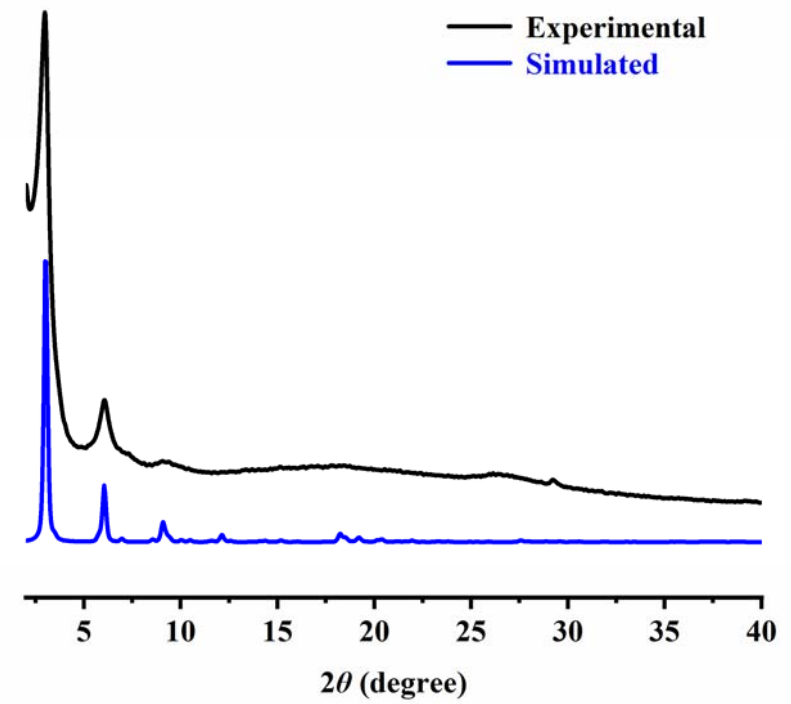

Figure S13. A comparison of experimental and simulated PXRD patterns of JUC-589 based on the **bcu** net.

Section S9. Gas adsorption

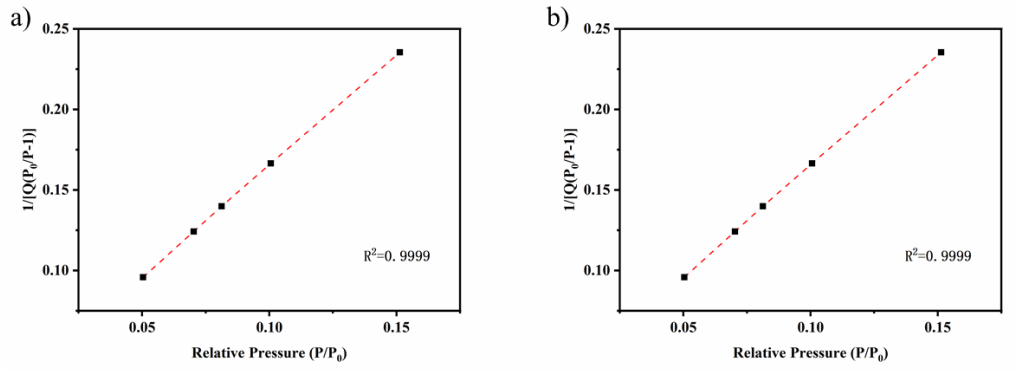

Figure S14. BET plots of JUC-588 (a) and JUC-589 (b) calculated from N_2 adsorption isotherms at 77 K.

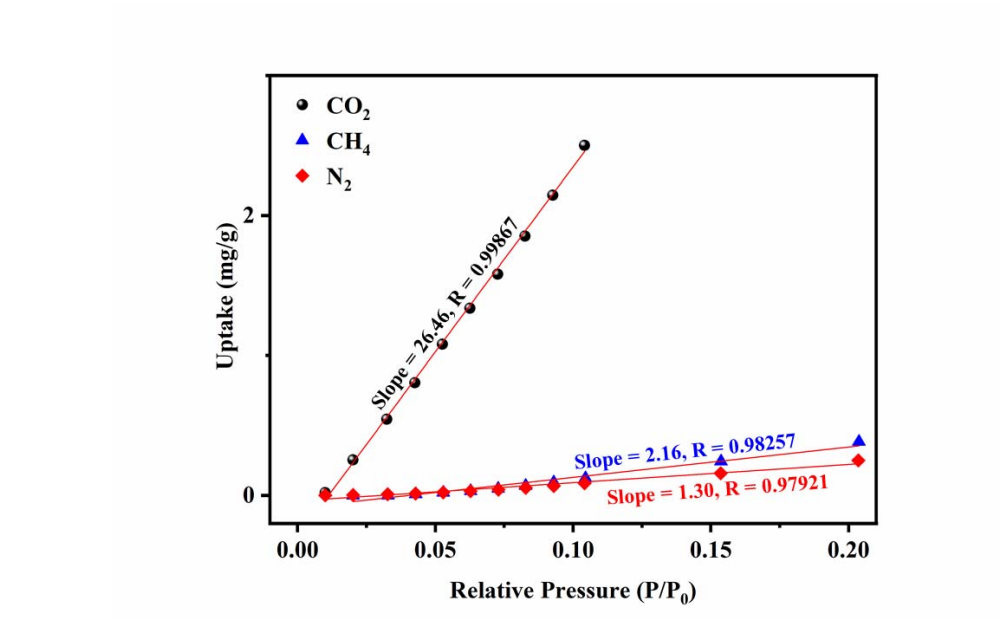

Figure S15. Linear fitting of the low-pressure Henry region of gas adsorption isotherms on JUC-588 measured at 273 K.

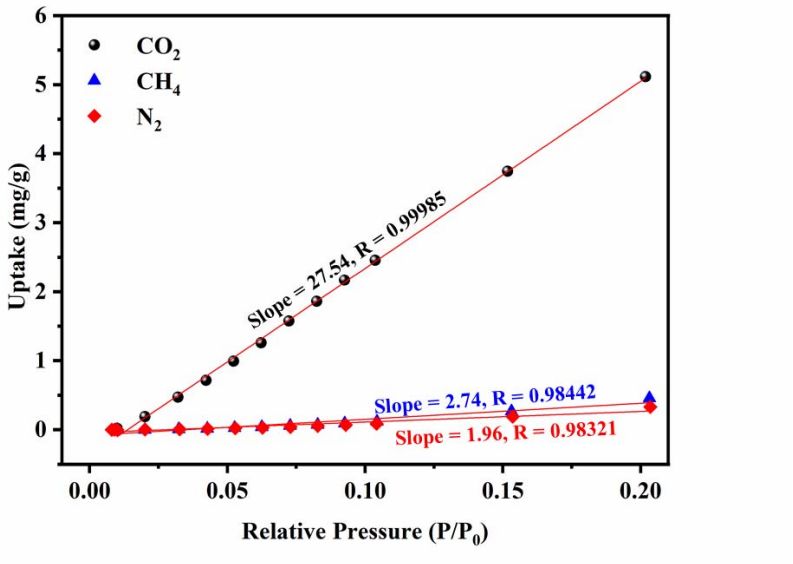

Figure S16. Linear fitting of the low-pressure Henry region of gas adsorption isotherms on JUC-589 measured at 273 K.

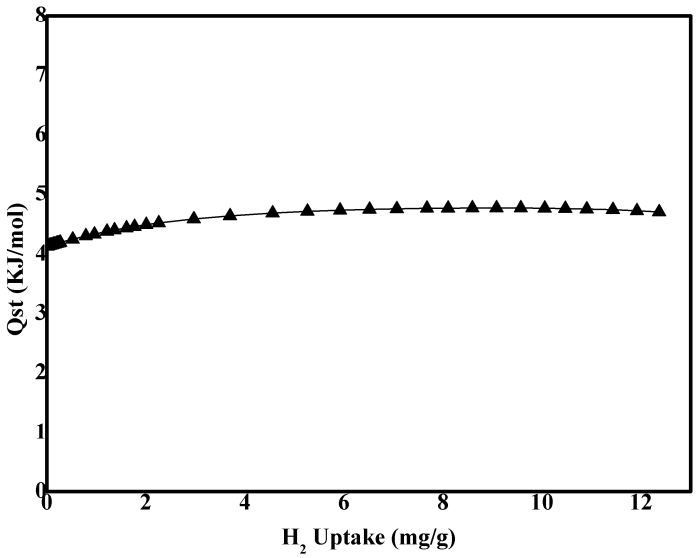

Figure S17. The experimental H_2 adsorption enthalpies (Q_{st}) of JUC-588.

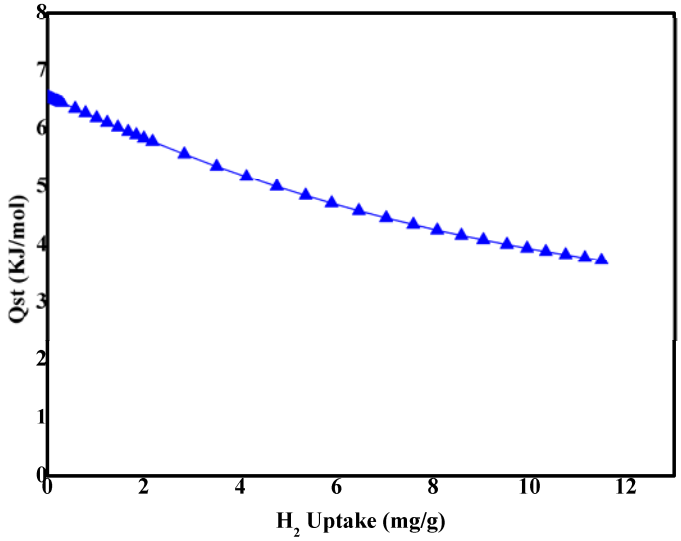

Figure S18. The experimental H_2 adsorption enthalpies (Q_{st}) of JUC-589.

Table 1 | Experimental and modelling results of gas adsorption on JUC-588 and JUC-589.

	BET	Pore volume	Pore size	Uptake ($cm^3\ g^{-1}$)			Ideal adsorption selectivity	
	(m^2g^{-1})	(cm^3g^{-1})	(Å)	CO_2	CH_4	N_2	CO_2/CH_4	CO_2/N_2
JUC-588	2728	3.21	17	67	16	6	12	20
JUC-589	2482	2.27	21	40	12	5	10	14

Table 2 | CH_4 uptakes for typical COFs, MOFs, POFs and porous carbons.

	CH_4 uptake (cm^3g^{-1}) at 273 K and 1 bar	Ref.
ACOF-1	16.1	4
ILCOF-1	12.6	6
TDCOF-5	14.98	5
COF-10	8.12	4
ICOF-2	64.68	11
COF-JLU2	53.2	12
COF-TpAzo	18.76	13
MCOF-1	9	14
Tg-AzoCOF	2	15
C_{10}-AzoCOF	2.6	15
H-AzoCOF	5.1	15
JUC-596	31	49
JUC-597	25	49
JUC-588	16	This work

JUC-589	12	This work
NJU-Bai$_{11}$	31.2	16
$Zn_4O(L)_2(NMP)_2(H_2O)]\cdot 2NMP\cdot 2H_2O$	7.8	17
$[Zn(HL)(bpe)_{0.5}]\cdot DMF\cdot H_2O$	4.5	17
$[Zn(HL)\text{-}(bipy)_{0.5}]\cdot DMF\cdot H_2O$	4.1	17
GDMU-2	19	18
$[Ni_2(\mu_2\text{-}OH)(bpdc)(tpt)_2][NO_3]\cdot 3DMA\cdot 4CH_3OH\cdot 6H_2O$	26	19
UPC-33	9.7	20
IITKGP-8	10.8	21
ZJU-15	15	22
UPC-32	31.3	23
ZIF-95	6.72	24
ZIF-95	6.94	24
$Ni(4\text{-}DPDS)_2CrO_4$	27.55	25
$\{[Cu(TIA)]\cdot 1.5CH_3OH\}_n$(Cu-1)	41.37	26
MPOP1	14.98	32
MPOP2	15.4	32
MPOP3	22.12	32
BDPCMP-1	10.75 (1.13 bar)	34
BDPCMP-2	15.68 (1.13 bar)	34
BDPCMP-3	13.44 (1.13 bar)	34
BDPCMP-4	12.54 (1.13 bar)	34
Cz-POF-1	32	35
Cz-POF-2	15.96	35
Cz-POF-3	35.56	35
Cz-POF-4	14.56	35
B-POF	13.8	36
P-POF	13.3	36
BP-POF	13.6	36
MPOF-Ad-1	21.0	37
MPOF-Ad-2	21.5	37
MPOF-Ad-3	13.7	37
BILP-5	21	38
CPC-550	60.2	38
CPC-600	51.8	38
CPC-650	49	38
CPC-700	47.6	38
CPC-800	44.8	38
WAPC	26.43	39
N-WAPC	15.0	39
PF-600 KOH	44.8	40
PF-800 KOH	50.8	40
PF-600 $ZnCl_2$	44.8	40
PF-800 $ZnCl_2$	47.4	40

PSK-1-550	36.28	41
PSK-2-650	49.28	41
PSK-3-750	32.92	41
SNMC-1-600	49.5	42
SNMC-2-600	55.5	42
SNMC-3-600	42.8	42
CSC2-700	47.9	43
CSC1-750	51.3	43
CSC2-750	58.4	43
CSC3-750	45.9	43
CSC2-800	53.7	43

Table 3 | CO_2 uptakes for typical COFs, MOFs, POFs and porous carbons.

	CO_2 uptake (cm^3g^{-1}) at 273 K and 1 bar	Ref.
ACOF-1	90.1	4
COF-5	30.03	4
COF-103	38.69	4
TDCOF-5	46.83	5
ILCOF-1	30.54	6
TPA-COF-3	46.4	10
TPA-COF-2	41.95	10
TPA-COF-6	47.03	10
TPA-COF-5	30.26	10
Tg-AzoCOF	15	15
C_{10}-AzoCOF	14	15
H-AzoCOF	21	15
JUC-596	84	49
JUC-597	70	49
JUC-588	67	This work
JUC-589	40	This work
NJU-Bai_{11}	130	16
$Zn_4O(L)_2(NMP)_2(H_2O)]\cdot 2NMP\cdot 2H_2O$	20.2	17
$[Zn(HL)(bpe)_{0.5}]\cdot DMF\cdot H_2O$	28.1	17
$[Zn(HL)\text{-}(bipy)_{0.5}]\cdot DMF\cdot H_2O$	17.7	17
GDMU-2	74	18
$[Ni_2(\mu_2\text{-}OH)(bpdc)(tpt)_2][NO_3]\cdot 3DMA\cdot 4CH_3OH\cdot 6H_2O$	108.2	19
UPC-33	68.1	20
IITKGP-8	55.4	21
ZJU-15	63	22
ZIF-95	20.16	24
ZIF-95	24.64	24
$\{[Cu(TIA)]\cdot 1.5CH_3OH\}_n$(Cu-1)	180.05	26
MPOP1	59.05	32

MPOP2	52.94	32
MPOP3	75.34	32
TPDC POPs P1	16	33
BDPCMP-1	37.632 (1.13 bar)	34
BDPCMP-2	50.4 (1.13 bar)	34
BDPCMP-3	45.47 (1.13 bar)	34
BDPCMP-4	42.78 (1.13 bar)	34
Cz-POF-1	102.8	35
Cz-POF-2	39.2	35
Cz-POF-3	106.9	35
Cz-POF-4	61.6	35
B-POF	46.0	36
P-POF	48.4	36
BP-POF	43.5	36
MPOF-Ad-1	69.5	37
MPOF-Ad-2	68.5	37
MPOF-Ad-3	46.0	37
BILP-5	65.16	38
CPC-550	186.8	38
CPC-600	168.5	38
CPC-650	151.2	38
CPC-700	130.83	38
CPC-800	120.14	38
WAPC	83.5	39
N-WAPC	100.8	39
PSK-1-550	75.04	41
PSK-2-650	118.27	41
PSK-3-750	92.06	41
SNMC-1-600	130.3	42
SNMC-2-600	165.3	42
SNMC-3-600	119.6	42
CSC2-700	97.4	43
CSC1-750	120.5	43
CSC2-750	148.1	43
CSC3-750	142.0	43
CSC2-800	102.4	43

Table 4 | H_2 uptakes for typical COFs, MOFs, POFs and porous carbons.

	H_2 uptake (cm^3g^{-1}) At 77 K and 1 bar	Ref.
ACOF-1	110.88	4
COF-10	91.84	4
COF-5	94.08	4
CoPc-PorDBA COF	89.6	7

COF-103	144.48	4
COF-18 Å	173.6	8
CTF-1	173.6	9
TDCOF-5	179.2	5
JUC-596	305	49
JUC-597	148	49
JUC-588	245	This work
JUC-589	211	This work
NJU-Bai_{11}	160.0	16
GDMU-2	240.7	18
$[Ni_2(\mu_2\text{-}OH)(bpdc)(tpt)_2][NO_3]\cdot 3DMA\cdot 4CH_3OH\cdot 6H_2O$	203.2	19
MOF-505	290.08	27
PCN-16	291.2	27
PCN-46	218.4	27
NOTT-101	282.24	27
NOTT-102	250.88	27
NJU-Bai12-ac	213.92	27
NU-111	232.96	28
Cu-BTC/GO	272.16	29
FJI-Y9-ht	202.3	30
FIR-29-ht	136.8	30
$Cu_{0.625}Ni_{0.375}(BDC)TED_{0.5}$	228.48	31
MOF-74(Mg)	246.4	31
MOF-5	212.8	31
MIL-101(Cr)	212.8	31
UIO-66	168	31
Cu-BTC	125.44	31
Zn-ZIF-8	141.12	31
MPOP1	98.56	32
MPOP2	112	32
MPOP3	107.52	32
TPDC POPs P1	68	33
BDPCMP-1	89.6 (1.13 bar)	34
BDPCMP-2	114.24 (1.13 bar)	34
BDPCMP-3	107.52 (1.13 bar)	34
BDPCMP-4	94.08 (1.13 bar)	34
Cz-POF-1	250.88	35
Cz-POF-2	108.64	35
Cz-POF-3	231.84	35
Cz-POF-4	115.36	35
B-POF	103.3	36
P-POF	102.8	36
BP-POF	100	36
CU-600	150.6	44

CT-600	185.1	44
CU-800	194.2	44
CT-800	267.3	44
AC-K5	278.8	45
AC-K4	142.2	45
AC-K3	249.7	45
AC-K2	190.4	45
AC	137.7	45
BG-S	170.12	46
NPC-1	234.18	47
NPC-2	278.88	47
NPC-3	316.96	47
NPC-4	320.32	47
CS-C	120.96	48
CS-SE	209.44	48
CS-AC	212.8	48
CS-AC-SE	227.36	48
CS-SE-AC	309.12	48

Section S10. Dye adsorption

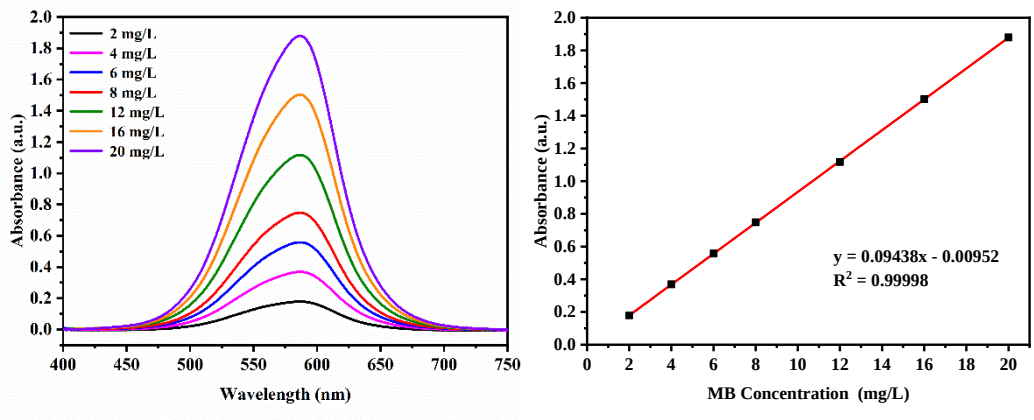

Figure S19. A standard curve of UV-Vis Spectrum for dye R250.

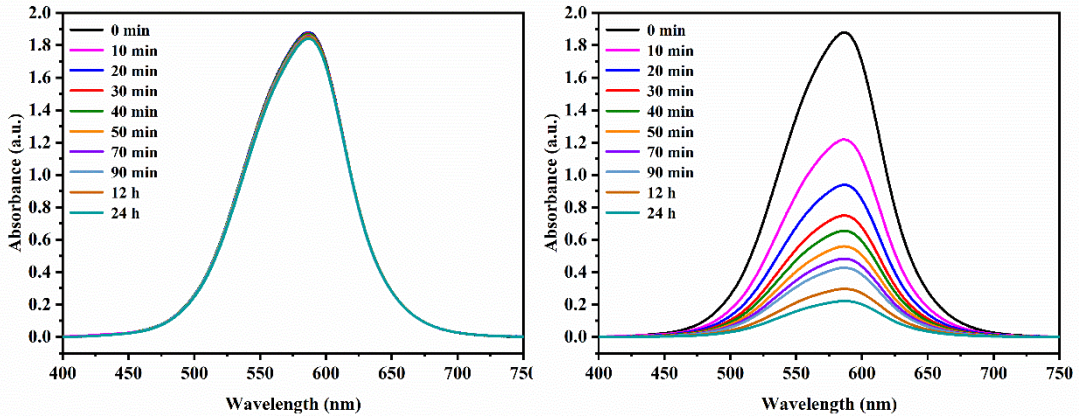

Figure S20. Adsorption of dye R250 for JUC-588 (left) and JUC-589 (right).

Section S11: Unit cell parameters and fractional atomic coordinates

Table S5. Unit cell parameters and fractional atomic coordinates for JUC-588 calculated based on the **bcu** net.

Space group		$P4_2/nmc$	
Calculated unit cell		$a = b = 23.819$ Å, $c = 23.9058$ Å, $\alpha = \beta = \gamma = 90°$	
Measured unit cell		$a = b = 23.835$ Å, $c = 23.9071$ Å, $\alpha = \beta = \gamma = 90°$	
Pawley refinement		$Rp = 2.86\%$, $Rwp = 3.76\%$	
atoms	x	y	z
C1	0.62698	0.54985	-0.32876
C2	0.67581	0.55153	-0.29673
C3	0.69267	0.38959	-0.28578
N4	0.7355	0.63062	-0.25889
C5	0.7426	0.3092	-0.25444
C6	0.27141	0.7041	0.27869
C7	0.28673	0.7886	0.2257
H8	0.60701	0.59147	-0.34136
H9	0.66588	0.35354	-0.30225
H10	0.28803	0.66608	0.30246
H11	0.31588	0.8207	0.20551
C12	0.5	0.5	-0.3494
C13	0.5	0.5	-0.46845
C14	0.5	0.5	0.28533
C15	0.55116	0.5	-0.37901
C16	0.60281	0.5	-0.34519
C17	0.5513	0.5	-0.43964
C18	0.70159	0.5	-0.27999
C19	0.65345	0.5	-0.45132
O20	0.59913	0.5	-0.47504

Table S6. Unit cell parameters and fractional atomic coordinates for JUC-589 calculated based on the **bcu** net.

Space group	*Immm*
Calculated unit cell	$a = 35.7099$ Å, $b = 9.7315$ Å, $c = 50.7873$ Å, $\alpha = \beta = \gamma = 90°$

Measured unit cell		a = 35.7110 Å, b = 9.7331 Å, c = 50.7884 Å, $\alpha = \beta = \gamma$ = 90°	
Pawley refinement		Rp = 1.12%, Rwp = 1.53%	
atoms	x	y	z
C1	0.58543	0.7049	0.60478
C2	0.5313	0.66408	0.56562
C3	0.67226	0.7312	0.66427
C4	0.61539	0.71816	0.62535
N5	0.69589	0.75789	0.70875
C6	0.70244	0.7303	0.68415
C7	0.72365	0.75472	0.72928
C8	0.47951	0.68112	0.59152
C9	0.4532	0.69915	0.61162
C10	0.4045	0.69509	0.5777
C11	0.43142	0.67232	0.55816
C12	0.34816	0.66905	0.62034
C13	0.32021	0.67641	0.6394
C14	0.36369	0.78319	0.66952
C15	0.39177	0.7776	0.6502
C16	0.23781	0.77111	0.72417
C17	0.28819	0.73498	0.75527
H18	0.73	0.69699	0.67796
H19	0.46267	0.70673	0.63177
H20	0.37585	0.70673	0.57128
H21	0.42339	0.66403	0.53767
H22	0.34093	0.62092	0.60189
H23	0.29269	0.63597	0.63483
H24	0.3701	0.82825	0.68849
H25	0.41887	0.82085	0.65483
H26	0.22761	0.79076	0.70449
H27	0.31769	0.72191	0.75954
N28	0.5	0.64854	0.54844
C29	0.5	0.57036	0.52436
C30	0.5	0.63519	0.5
N31	0.5	0.88382	0.5
C32	0.5	0.77037	0.5

Section S12. References

(1) V. Abet, F. T. Szczypinski, M. A. Little, V. Santolini, C. D. Jones, R. Evans, C. Wilson, X. Wu, M. F. Thorne, M. J. Bennison, P. Cui, A. I. Cooper, K. E. Jelfs and A. G. Slater, Angew Chem Int Edit, 2020, **59**, 20272-20272.

(2) W. G. Lu, Z. W. Wei, D. Q. Yuan, J. Tian, S. Fordham and H. C. Zhou, *Chem Mater*, 2014, **26**, 4589-4597.

(3) J W. Li, Y. W. Ren, C. R. Qi and H. F. Jiang, *Eur J Inorg Chem*, 2017, **11**, 1478-1487.

(4) Z. P. Li, X. Feng, Y. C. Zou, Y. W. Zhang, H. Xia, X. M. Liu and Y. Mu, *Chem Commun*, 2014, **50**, 13825-13828.

(5) Z. Kahveci, T. Islamoglu, G. A. Shar, R. Ding and H. M. El-Kaderi, *Crystengcomm*, 2013, **15**, 1524-1527.

(6) M. G. Rabbani, A. K. Sekizkardes, Z. Kahveci, T. E. Reich, R. S. Ding and H. M. El-Kaderi, *Chem-Eur J*, 2013, **19**, 3324-3328.

(7) V. S. P. K. Neti, X. F. Wu, S. G. Deng and L. Echegoyen, *Crystengcomm*, 2013, **15**, 6892-6895.

(8) R. W. Tilford, S. J. Mugavero, P. J. Pellechia and J. J. Lavigne, *Adv Mater*, 2008, **20**, 2741-2746.

(9) P. Kuhn, M. Antonietti and A. Thomas, *Angew Chem Int Edit*, 2008, **47**, 3450-3453.

(10) A. F. M. El-Mahdy, C. H. Kuo, A. Alshehri, C. Young, Y. Yamauchi, J. Kim and S. W. Kuo, *Journal of Materials Chemistry A*, 2018, **6**, 19532-19541.

(11) Y. Du, H. S. Yang, J. M. Whiteley, S. Wan, Y. H. Jin, S. H. Lee and W. Zhang, *Angew Chem Int Edit*, 2016, **55**, 1737-1741.

(12) Z. P. Li, Y. F. Zhi, X. Feng, X. S. Ding, Y. C. Zou, X. M. Liu and Y. Mu, *Chem-Eur J*, 2015, **21**, 12079-12084.

(13) R. Ge, D. D. Hao, Q. Shi, B. Dong, W. G. Leng, C. Wang and Y. N. Gao, *J Chem Eng Data*, 2016, **61**, 1904-1909.

(14) H. P. Ma, H. Ren, S. Meng, Z. J. Yan, H. Y. Zhao, F. X. Sun and G. S. Zhu, *Chem Commun*, 2013, **49**, 9773-9775.

(15) S. F. Huang, Y. M. Hu, L. L. Tan, S. Wan, S. Yazdi, Y. H. Jin and W. Zhang, *Acs Appl Mater Inter*, 2020, **12**, 51517-51522.

(16) K. Z. Tang, R. R. Yun, Z. Y. Lu, L. T. Du, M. X. Zhang, Q. Wang and H. Y. Liu, *Cryst Growth Des*, 2013, **13**, 1382-1385.

(17) Y. Zhao, L. Wang, N. N. Fan, M. L. Han, G. P. Yang and L. F. Ma, *Cryst Growth Des*, 2018, **18**, 7114-7121.

(18) J. Q. Liu, G. L. Liu, C. Y. Gu, W. C. Liu, J. W. Xu, B. H. Li and W. J. Wang, *Journal of Materials Chemistry A*, 2016, **4**, 11630-11634.

(19) L. Zhang, J. J. Qian, W. B. Yang, X. F. Kuang, J. Zhang, Y. X. Cui, W. M. Wu, X. Y. Wu, C. Z. Lu and W. Z. Chen, *Journal of Materials Chemistry A*, 2015, **3**, 15399-15402.

(20) W. D. Fan, Y. T. Wang, Q. Zhang, A. Kirchon, Z. Y. Xiao, L. L. Zhang, F. N. Dai, R. M. Wang and D. F. Sun, *Chem-Eur J*, 2018, **24**, 2137-2143.

(21) S. Chand, A. Pal and M. C. Das, *Chem-Eur J*, 2018, **24**, 5982-5986.

(22) . Duan, Y. Zhou, R. Lv, B. Yu, H. D. Chen, Z. G. Ji, Y. J. Cui, Y. Yang and G. D. Qian, *J Solid State Chem*, 2018, **260**, 31-33.

(23) W. D. Fan, Y. T. Wang, Z. Y. Xiao, Z. D. Huang, F. N. Dai, R. M. Wang and D. F. Sun, *Chinese Chem Lett*, 2018, **29**, 865-868.

(24) Z. H. Rada, H. R. Abid, H. Q. Sun, J. Shang, J. Y. Li, Y. D. He, S. M. Liu and S. B. Wang, *Prog Nat Sci-Mater*, 2018, **28**, 160-167.

(25) F. Zheng, L. H. Chen, R. D. Chen, Z. G. Zhang, Q. W. Yang, Y. W. Yang, B. G. Su, Q. L. Ren and Z. B. Bao, *Sep Purif Technol*, 2022, **281**, 119911.

(26) Z. L. Ma, P. X. Liu, Z. Y. Liu, J. J. Wang, L. B. Li and L. Tian, *Inorg Chem*, 2021, **60**, 6550-6558.

(27) B. S. Zheng, R. R. Yun, J. F. Bai, Z. Y. Lu, L. T. Du and Y. Z. Li, *Inorg Chem*, 2013, **52**, 2823-2829.

(28) S. Suepaul, K. A. Forrest, T. Pham and B. Space, *Cryst Growth Des*, 2018, **18**, 7599-7610.

(29) A. M. Varghese, K. S. K. Reddy and G. N. Karanikolos, *Ind Eng Chem Res*, 2022, **61**, 6200-6213.

(30) F. J. Zhao, Y. X. Tan, W. J. Wang, Z. F. Ju and D. Q. Yuan, *Inorg Chem*, 2018, **57**, 13312-13317.

(31) R. J. Li, X. Han, Q. N. Liu, A. Qian, F. F. Zhu, J. W. Hu, J. Fan, H. T. Shen, J. C. Liu, X. Pu, H. T. Xu and B. Mu, *Acs Omega*, 2022, **7,** 20081-20091.

(32) G. Li, Q. Q. Liu, B. J. Xia, J. Huang, S. Z. Li, Y. Z. Guan, H. Zhou, B. Liao, Z. H. Zhou and B. Liu, *Eur Polym J*, 2017, **91**, 242-247.

(33) S. Bandyopadhyay, P. Pallavi, A. G. Anil and A. Patra, *Polym Chem-Uk*, 2015, **6**, 3775-3780.

(34) Y. F. Xu, D. Chang, S. Feng, C. Zhang and J. X. Jiang, *New J Chem*, 2016, **40**, 9415-9423.

(35) X. Zhang, J. Z. Lu and J. Zhang, *Chem Mater*, 2014, **26**, 4023-4029.

(36) G. L. Xing, T. T. Yan, S. Das, L. Ye and K. Q. Ye, *Rsc Adv*, 2018, **8**, 20434-20439.

(37) W. Q. Wen, P. S. Shuttleworth, H. B. Yue, J. P. Fernandez-Blazquez and J. W. Guo, *Acs Appl Mater Inter*, 2020, **12**, 7548-7556.

(38) B. Ashourirad, A. K. Sekizkardes, S. Altarawneh and H. M. El-Kaderi, *Chem Mater*, 2015, **27**, 1349-1358.

(39) Y. Li, R. Xu, B. B. Wang, J. P. Wei, L. Y. Wang, M. Q. Shen and J. Yang, *Nanomaterials-Basel*, 2019, **9**, 266.

(40) J. Wang, R. Krishna, X. F. Wu, Y. Q. Sun and S. G. Deng, *Langmuir*, 2015, **31**, 9845-9852.

(41) Y. Zhang, Z. Q. Wei, X. Liu, F. Liu, Z. H. Yan, S. Y. Zhou, J. Wang and S. G. Deng, *Rsc Adv*, 2022, **12**, 8592-8599.

(42) P. X. Zhang, Y. Zhong, J. Ding, J. Wang, M. Xu, Q. Deng, Z. L. Zeng and S. G. Deng, *Chemical Engineering Journal*, 2019, **355**, 963-973.

(43) C. C. Song, W. Y. Ye, Y. C. Liu, H. Huang, H. Zhang, H. Lin, R. W. Lu and S. F. Zhang, *Acs Omega*, 2020, **5**, 28255-28263.

(44) D. D. Wang, Y. L. Shen, Y. L. Chen, L. L. Liu and Y. F. Zhao, *Chem. Eng. J.*, 2019, **367**, 260-268.

(45) H. L. Wang, Q. M. Gao and J. Hu, *J. Am. Chem. Soc.*, 2009, **131**, 7016-7022.

(46) H. Y. Zhang, Y. W. Zhu, Q. Y. Liu and X. W. Li, *Appl Energ*, 2022, **306**.

(47) R. Mishra, P. R. Prasad, P. Panda and S. Barman, *Energ Fuel*, 2021, **35**, 14177-14187.

(48) J. H. Park and S. J. Park, *Carbon*, 2020, **158**, 364-371.

(49) C. Y. Yu, H. Li, Y. J. Wang, J. Q. Suo, X. Y. Guan, R. Wang, V. Valtchev, Y. S. Yan, S. L. Qiu,

Q. R. Fang, *Angew. Chem. Int. Ed.,* 2022, **61**, e202117101.